

This work was written as part of one of the author's official duties as an Employee of the United States Government and is therefore a work of the United States Government. In accordance with 17 U.S.C. 105, no copyright protection is available for such works under U.S. Law. Access to this work was provided by the University of Maryland, Baltimore County (UMBC) ScholarWorks@UMBC digital repository on the Maryland Shared Open Access (MD-SOAR) platform.

Please provide feedback

Please support the ScholarWorks@UMBC repository by emailing scholarworks-group@umbc.edu and telling us what having access to this work means to you and why it's important to you. Thank you.

Broadband super-resolving lens with high transparency in the visible range

Cite as: Appl. Phys. Lett. **90**, 174113 (2007); <https://doi.org/10.1063/1.2734496>

Submitted: 08 November 2006 . Accepted: 04 April 2007 . Published Online: 27 April 2007

M. Bloemer, G. D'Aguanno, N. Mattiucci, M. Scalora, and N. Akozbek



View Online



Export Citation

ARTICLES YOU MAY BE INTERESTED IN

[Limitations on subdiffraction imaging with a negative refractive index slab](#)

Applied Physics Letters **82**, 1506 (2003); <https://doi.org/10.1063/1.1554779>

[Microwave transmission through a two-dimensional, isotropic, left-handed metamaterial](#)

Applied Physics Letters **78**, 489 (2001); <https://doi.org/10.1063/1.1343489>

[Transparent, metallo-dielectric, one-dimensional, photonic band-gap structures](#)

Journal of Applied Physics **83**, 2377 (1998); <https://doi.org/10.1063/1.366996>

Lock-in Amplifiers
up to 600 MHz



Broadband super-resolving lens with high transparency in the visible range

M. Bloemer,^{a)} G. D'Aguanno, N. Mattiucci, M. Scalora, and N. Akozbek
 Department of the Army, Charles M. Bowden Facility, Bldg. 7804, Research, Development, and
 Engineering Command, Redstone Arsenal, Alabama 35898

(Received 8 November 2006; accepted 4 April 2007; published online 27 April 2007)

The authors present a theoretical analysis of a super-resolving lens based on one-dimensional metal-dielectric photonic band gap composed of Ag/GaP multilayers. The lens contains a total of ten optical skin depths of Ag, yet maintains a normal incidence transmittance of $\sim 50\%$ for propagating waves over the super-resolving wavelength range of 500–650 nm. The individual Ag layers are 22 nm thick and can be readily fabricated in conventional deposition systems. The importance of antireflection coatings for the transmission of evanescent and propagating waves is illustrated by comparison to periodic and symmetric structures without the coatings. © 2007 American Institute of Physics. [DOI: 10.1063/1.2734496]

In the year 2000, Pendry¹ showed that a simple metal film displayed negative refraction of the Poynting vector for TM polarized light and was capable of supporting evanescent waves. This unique combination resulted in a flat superlens that could image an object with a resolution beyond traditional glass lenses which support only propagating waves. The performance limit of the metallic superlens was associated with the losses in the metallic film.

In order to overcome the losses associated with a single metal film, Ramakrishna *et al.*² designed a superlens based on a multilayer metal-dielectric stack having thin metal layers. This combination of a positive and negative dielectric constant material results in a slightly different type of superlens. Instead of having a focus inside of the metal film, this geometry balanced the negative and positive refraction of the Poynting vector in consecutive layers, leading to a waveguide-type effect that carries the propagating waves through the structure without the usual diffraction.

Since the introduction of the metal-dielectric superlens, there have been numerous attempts to design structures with high transmittance for the evanescent waves.^{3–6} However, very little has been said about the transmittance of the propagating waves and the bandwidth of the lens. In the following we start with a metal-dielectric structure known to have broadband and high transmittance for the propagating waves. The structure we examine is a one-dimensional metal-dielectric photonic band gap (1D MDPBG) based on Ag/GaP. These 1D MDPBGs are known to have a very low sheet resistance ($\sim 0.1 \Omega/\text{sq}$) due to the high fraction of metal in the multilayer stack.⁷ In general, most of the interest in photonic crystals has concentrated on the unique properties of the band gap and the band edges, but for MDPBG the interest is on the passband precisely because of the unusual combination of broadband, high transmittance, and high electrical conductivity, hence they are often called “transparent metals.”

The concept of a transparent MDPBG is based on a series of strongly coupled metal-dielectric Fabry-Pérot cavities.⁸ As an example, we start with a single cavity of Ag/GaP/Ag (22 nm/35 nm/22 nm) surrounded by air. Normally, the lowest order transmission resonance occurs at the

half-wave condition; however, the phase change upon reflection needs to be explicitly included in the interference equation.⁹ The departure from a perfect reflector can be substantial, and in the case of our Ag/GaP/Ag cavity, the optical thickness of the GaP is closer to a quarter wave. The normal incidence transmittance for the Fabry-Pérot cavity shown in Fig. 1 displays a resonance at a wavelength of 570 nm. The transmittance was calculated using a standard matrix transfer method and the optical constants of Ag and GaP were taken from Palik.¹⁰ The optical constants of Ref. 10 were measured from bulk materials and the experimental losses for thin films may be larger than predicted here.

Adding another period of GaP/Ag results in two coupled cavities and removes the degeneracy, causing the single resonance at 570 nm to split into two resonances at 490 and 620 nm. The amount of the splitting depends on the thickness of the Ag layers, with thinner layers providing a larger separation in the transmission resonances. Adding another period results in three coupled cavities and three resonances and so on for more periods. Figure 1 also shows the transmittance for five coupled cavities or 5.5 periods of Ag/GaP (22 nm/35 nm). The details of the transmittance are strongly influenced by the dispersion of the Ag.⁷ The most important feature to note in comparing the transmittance of the single cavity and five coupled cavities is the high degree of trans-

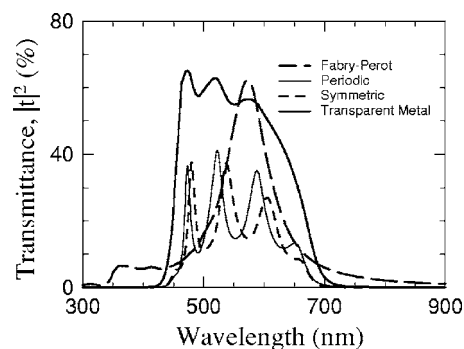


FIG. 1. Normal incidence transmittance of a single Fabry-Pérot cavity, Ag/GaP/Ag (22 nm/35 nm/22 nm), periodic MDPBG [6 periods of Ag/GaP (22 nm/35 nm)], a symmetric MDPBG [5.5 periods of Ag/GaP (22 nm/35 nm)], and a transparent metal MDPBG [5.5 periods of Ag/GaP (22 nm/35 nm) with 17 nm thick GaP AR coatings on the entrance and exit faces].

^{a)}Electronic mail: mbloemer@pclnet.net

parency in spite of the five cavity structure having ~ 10 optical skin depths of metal compared to ~ 3.5 optical skin depths for the single cavity. The high transparency is attributed to resonance tunneling through coupled cavities.

While the transmittance of the 5.5 period MDPBG is large, it can be improved by the addition of antireflection coatings. It was found that the antireflection (AR) coating designed for a single metal-dielectric Fabry-Pérot cavity¹¹ worked equally well for coupled cavities.¹² The AR coating is simply $\frac{1}{2}$ the thickness of the dielectric spacer and of the same material. The AR coatings double the overall transmittance and smooth out the oscillations associated with the coupled cavity modes.

The angular dependence of the transmittance spectra in Fig. 1 depends strongly on the refractive index of the dielectric spacer. As the angle of incidence increases, the passband shifts towards the blue, but the large refractive index of GaP (~ 3.5) reduces the change in the optical path with angle by causing the rays to stay close to the normal. The high refractive index also improves the overall transmittance of the MDPBG.

In the following we will examine the transmission characteristics for the evanescent waves and the superlensing properties of the MDPBG of Fig. 1. We compare three geometries, a periodic MDPBG, a symmetric MDPBG, and a transparent metal MDPBG. All three structures have the same amount of Ag, 132 nm total thickness equally divided into six layers. Similar to the transmittance spectra of Fig. 1 for the propagating waves, the three different MDPBGs have drastically different transmittance for the evanescent waves due to the first and last layers of the structures.

The calculations of the lensing properties of MDPBG have been carried out using the technique of the angular spectrum decomposition¹³ in conjunction with the transfer matrix technique. A plane, monochromatic, TM polarized wave with wave vector k_0 in free space is incident on the object plane which is at a distance d from the input surface of a MDPBG lens of length L . Note that both the object plane and the lens are in free space. The magnetic field is expressed as

$$\mathbf{H}(x, z, t) = (1/2)[\tilde{\mathbf{H}}(x, z)e^{-i\omega t} + \text{c.c.}], \quad (1)$$

where $\tilde{\mathbf{H}}(x, z) = \tilde{H}(x, z)\hat{y}$ is the complex, stationary vector field, \hat{y} is the unit vector of the y axis, and the z axis is normal to the layers of the MDPBG. The complex amplitude of the magnetic field $\tilde{H}(x, z)$ at $z \geq L$ (i.e., in the semispace at the output of the lens) is expressed by the following integral:

$$\tilde{H}(x, z \geq L) = \int_{-\infty}^{+\infty} A(k_x)t(k_x)e^{ik_x x}e^{i\sqrt{k_0^2 - k_x^2}(z+d-L)}dk_x. \quad (2)$$

Here $A(k_x)$ is the Fourier spectrum of the magnetic field on the object plane, and $t(k_x)$ is the complex transmission function of the layered lens for TM polarization. The transmission function has been calculated using a matrix transfer technique.¹⁴ The diffraction limited field is obtained by removing the evanescent components and extending the integral only over the propagating modes. The electric field at $z \geq L$ has been calculated from the magnetic field using the relation $\nabla \times \tilde{\mathbf{H}} = -i\omega\epsilon_0\tilde{\mathbf{E}}$. Finally, the time averaged Poynting vector is obtained through the following formula: $\mathbf{S} = (1/2)\text{Re}[\tilde{\mathbf{E}}^* \times \tilde{\mathbf{H}}]$.

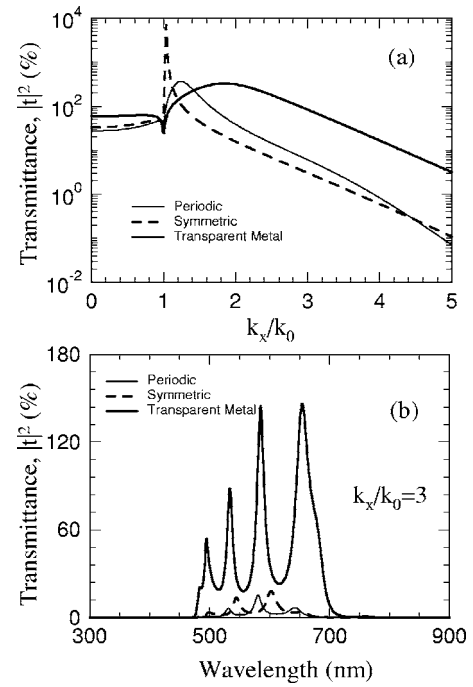


FIG. 2. (a) Transmittance of the Fourier components at a wavelength of 532 nm. (b) Transmittance vs wavelength for a single Fourier component at $k_x/k_0=3$.

The transmittance of the MDPBG is plotted in Fig. 2(a) as a function of k_x/k_0 at a wavelength of 532 nm and in Fig. 2(b) as a function of the wavelength for a value of $k_x/k_0=3$. In Fig. 2(a) we see that the symmetric MDPBG has a very high transmittance for Fourier components just beyond $k_x/k_0=1$, but it occurs over a very limited range. The periodic MDPBG has a slightly broader transmittance for the evanescent components with a peak at $k_x/k_0=1.25$. In comparison, the transparent metal MDPBG has a much broader range of k_x/k_0 values with good transmittance.

Figure 2(b) gives an indication of the broadband nature of the transparent metal MDPBG lens. Plotted is the transmittance for $k_x/k_0=3$. Without question, the transparent metal MDPBG has a significantly higher transmittance for this particular Fourier component compared with the symmetric or periodic MDPBG.

Figure 3 is a three-dimensional (3D) plot of the transmittance versus wavelength and k_x/k_0 . To save space we plot the 3D transmittance only for the transparent metal MDPBG and the periodic MDPBG. The symmetric MDPBG is only slightly better than the periodic MDPBG. The notable feature in Fig. 3 is the broadband, high transmittance of the propagating and evanescent waves for the transparent metal MDPBG. The five resonances associated with the five coupled cavities are clearly evident. Similar to the propagating waves, the transmittance of the evanescent waves is assisted by high index dielectric layers in providing a match in the magnitude of the dielectric constant of the metal, thereby reducing the reflections at the metal-dielectric boundary to allow greater penetration of the field throughout the structure. It also pulls the plasmonic guided modes toward higher values of k_x/k_0 .

The evanescent waves in the superlensing process involving metals are related to low group velocity surface plasmon modes. These surface plasmons propagate parallel to the metal-dielectric interfaces. The transverse boundaries

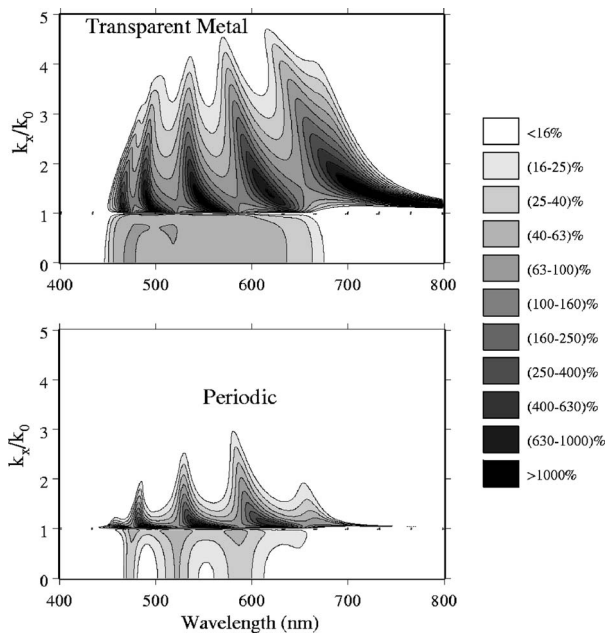


FIG. 3. Topographic three-dimensional plot of the transmittance vs wavelength and k_x/k_0 for the transparent metal MDPBG and the periodic MDPBG. The lowest contour line indicates a transmittance of 16%. Note that the contour lines are not uniformly spaced to include the wide range of transmittance values.

that define the surface plasmon guiding conditions are the same boundaries that determine the transmittance of the propagating waves, and the mathematical expression for the transmittance of the propagating waves is the same as for the evanescent waves. The passbands for the propagating and evanescent waves do not overlap perfectly, but the overlap is sufficient to provide a 150 nm wavelength band having super-resolving properties. A recent publication examines a transparent metal structure at a wavelength where the transmittance for the propagating waves is large and the transmittance of the evanescent waves is small.¹⁵

A transmittance of 100% for the evanescent components is not an indicator that the loss is zero. In fact, there are significant losses associated with surface plasmons at a metal-dielectric interface. While the power transferred into the far field is the same with and without evanescent components, the power loss is greater when the evanescent components excite surface plasmons.

The superlensing properties were examined by imaging two slits separated by less than $\lambda/2$ in free space. As an example, we look at a wavelength of 532 nm and compare all three MDPBGs. Figure 4 shows the image formed by the three lenses and also the case of the transparent metal MDPBG, but without evanescent components (diffraction limited). The slits (40 nm wide with a center to center spacing of 140 nm) are placed at the entrance of the lens (but in free space) and the image plane is located 50 nm beyond the end face of each lens. Although each lens contains six, 22 nm thick Ag films, the lenses have slightly different lengths due to the different geometries. The result is that the distance from the object plane to the image plane is 357, 391, and 392 nm for the symmetric, transparent metal, and periodic MDPBGs, respectively. The transparent metal MDPBG provides >95% contrast for the two slits at a slit separation of $\lambda/4$. The other two lenses are only slightly better than the diffraction limited case.

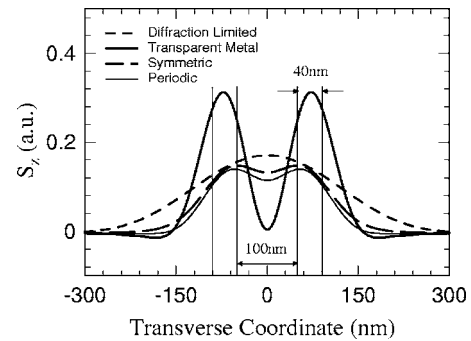


FIG. 4. Image formed by the lenses for two slit sources at a wavelength of 532 nm. The center to center slit separation is $\lambda/4$. The image plane is 50 nm from the end of the lens. The diffraction limited case is for the transparent metal but without the evanescent components included in the calculation.

It has been noted previously that the interference of propagating waves and evanescent waves can cause circulation in the Poynting vector.⁵ Remnants of the vortices can be seen in Fig. 4 for the slightly negative components of S_z at a distance of ~ 200 nm from the center of the slits. The presence of vortices is an indication that evanescent waves are contributing to the resolution of the lens.

Images similar to those shown in Fig. 4 were calculated throughout the transparency band of the transparent metal lens. It was found that over the wavelength range of 500–650 nm, the transparent metal lens could resolve two 40 nm wide slits with a contrast >80% and slit separation of $< \lambda/2.5$, where λ is the free space wavelength for the incident radiation. At most wavelengths, the slit separation was $\sim \lambda/4$. In addition, the transmittance for the normal incidence propagating waves was $\sim 50\%$ over the superlensing band (Fig. 1).

As a final note, the diffraction of the propagating waves is suppressed by the waveguiding in the metal/dielectric structure. The positive refraction of the Poynting vector in the dielectric is balanced by the negative refraction of the Poynting vector in the metal. Ag and GaP are dispersive but the balance is maintained over a large wavelength range by the large magnitudes of the dielectric constants for both the Ag and GaP, which cause the refraction angle to be small, even for large angles of incidence.

¹J. B. Pendry, Phys. Rev. Lett. **85**, 3966 (2000).

²S. A. Ramakrishna, J. B. Pendry, M. C. K. Wiltshire, and W. J. Stewart, J. Mod. Opt. **50**, 1419 (2003).

³H. Shin and S. Fan, Appl. Phys. Lett. **89**, 151102 (2006).

⁴B. Wood, J. B. Pendry, and D. P. Tsai, Phys. Rev. B **74**, 115116 (2006).

⁵K. J. Webb and M. Yang, Opt. Lett. **31**, 2130 (2006).

⁶S. Feng and J. M. Elson, Opt. Express **14**, 216 (2006).

⁷M. J. Bloemer and M. Scalora, Appl. Phys. Lett. **72**, 1676 (1998).

⁸M. Scalora, M. J. Bloemer, A. S. Pethel, J. P. Dowling, C. M. Bowden, and A. S. Manka, J. Appl. Phys. **83**, 2377 (1998).

⁹J. M. Bennett, J. Opt. Soc. Am. **54**, 612 (1964).

¹⁰Handbook of Optical Constants of Solids, edited by E. D. Palik ((Academic, New York, 1985), Vol. 1, pp. 350 and 445).

¹¹B. Bates and D. J. Bradley, Appl. Opt. **5**, 971 (1966).

¹²M. Scalora, M. J. Bloemer, and C. M. Bowden, Opt. Photonics News **10**, 23 (1999).

¹³L. Mandel and E. Wolf, *Optical Coherence and Quantum Optics* (Cambridge University Press, Cambridge, 1995), Vol. 1, p. 109.

¹⁴A. Yariv and P. Yeh, *Optical Waves in Crystals* (Wiley, New York, 1984), Vol. 1, p. 165.

¹⁵M. Scalora, G. D'Aguzzo, N. Mattiucci, M. Bloemer, D. de Ceglia, M. Centini, A. Mandatori, C. Sibilia, N. Akozbek, M. Cappeddu, M. Fowler, and J. W. Haus, Opt. Express **15**, 508 (2007).